EPJ Web of Conferences **319**, 03001 (2025) https://doi.org/10.1051/epjconf/202531903001
RICAP-24

Early clustering of DM particles around PBHs Density profiles and signatures

Pierre Salati[1,*] and *Julien* Lavalle[2,**]

[1]Université Grenoble Alpes, USMB, CNRS, LAPTh, 9 chemin de Bellevue, Annecy-le-Vieux, F-74941 Annecy, France

[2]Laboratoire Univers et Particules de Montpellier (LUPM), Université de Montpellier & CNRS, Place Eugène Bataillon, 34095 Montpellier Cedex 05, France

Abstract. Primordial black holes may have been produced in the early stages of the universe, after cosmic inflation. If so, dark matter in the form of elementary particles can be subsequently accreted around these objects, in particular when it gets non-relativistic and further streams freely in the primordial plasma. A dark matter mini-spike builds up gradually around each black hole during the radiation dominated era, with density orders of magnitude larger than the cosmological one. The radial profiles of mini-spikes depend sensitively on black hole mass, dark matter particle mass and temperature of kinetic decoupling. They exhibit a rich variety of behaviors which are presented here. These spikes subsequently annihilate and leave potentially detectable signatures in the extragalactic γ-ray background and in the cosmic microwave background.

1 From early ideas to the search of evidence

Primordial black holes (PBHs) emerged as a theoretical idea more than fifty years ago [1, 2]. These objects do not result from stellar activity. They are produced during the Big Bang by the collapse of primordial density perturbations extending over the scale of the horizon [3]. How PBHs actually form in the early universe is still a matter of debate. The magnitude of density perturbations required to seed a PBH is unnaturally large. That is why, although there were proposed to explain the astronomical dark matter (DM) as early as 1975 [4], PBHs did not attract much attention when the field started to bubble with activity in the 80's. At that time, ideas like supersymmetry or supergravity were considered as more attractive. They were based on fundamental principles, were falsifiable contrary to PBHs, and led to the existence of a natural DM candidate in the form of a stable, weakly interacting and massive particle dubbed WIMP.

Alas, after thirty years of an intense hunt at the accelerators LEP and LHC, WIMPs have not yet been discovered. This puts significant pressure on the models although alternative solutions have been suggested, based for instance on the existence of a mediator between the standard and dark sectors of the theory. There is also a plethora of other DM candidates such as sterile neutrinos or axions which are very well motivated from a theoretical point of view and that are actively sought after.

*e-mail: pierre.salati@lapth.cnrs.fr
**e-mail: lavalle@in2p3.fr

The revival of PBHs occurred when the first binary black hole merger was observed together with gravitational waves [5]. Black holes stopped suddenly to be a theoretical fantasy and entered the realm of almost direct observation. The fact that the merging objects were heavier than expected renewed the interest into PBHs as potential DM candidates and gave a fresh start to the field [6–8]. Many bounds apply though on the fraction $f_{\rm BH}$ of DM in the form of PBHs. Very light PBHs must have evaporated by now and cannot contribute to DM. At the other end of the mass spectrum, several mechanisms yield upper limits on $f_{\rm BH}$, some of which fairly stringent[1]. Only PBHs in the asteroid window, i.e. with masses in the range from 10^{17} to 10^{22} grams, are still allowed to make all the DM.

In this context, it is legitimate to explore more complex situations where DM is made of several components. In this article, we study the case where both PBHs and WIMP-like species contribute to DM. Very surprisingly, such a mixture is highly constrained by observations [12]. Both components cannot coexist in comparable amounts. Actually PBHs accrete WIMPs during the radiation dominated era to build ultra-compact mini-haloes around them. Inside these, the density of DM particles is so large that the resulting annihilation signals become visible, hence setting strong upper limits on $f_{\rm BH}$, in particular in the asteroid window. The density profiles of these DM mini-haloes need to be correctly derived though. This has only been recently developed in [13], revising the original study first carried out by [14]. The salient features and conclusions of this work are presented here, together with the bounds on the PBH abundance $f_{\rm BH}$. We might even go a step further and invert the reasoning. Gravitational wave observatories target sub-solar objects. The discovery of such PBHs with the measurement of their abundance $f_{\rm BH}$ would yield this time constraints on the WIMP properties.

2 Dressing of primordial black holes with thermal dark matter

Thermal particles are captured by a PBH if three conditions are met. To start with, the DM species should feel the gravitational pull of the black hole, i.e. they should lie in its sphere of influence. They should also be able to move freely inside the primordial plasma without colliding on its constituents. Finally, their velocities should not exceed the local escape velocity from the PBH. The last condition translates into a mechanical energy being negative.

2.1 Radius of influence of a black hole in the radiation dominated era

In the vacuum, the radius of gravitational influence of a PBH extends to infinity. In a plasma with non-vanishing energy density $\rho_{\rm tot}$, though, the sphere of influence is filled with a medium inside which the PBH is all the more swamped as the sphere is large. We can naively consider that the gravitational pull of the PBH becomes negligible when the mass of the plasma exceeds the PBH mass $M_{\rm BH}$. A more refined argument [15] is based on the acceleration of a test particle moving radially with the expanding plasma and feeling the PBH gravitational drag. The turn-around radius of the trajectory is identified with the radius of influence $r_{\rm inf}$. In a radiation dominated cosmology, trajectories are scale-invariant, hence the definition

$$M_{\rm BH} = \frac{16\pi}{3\eta_{\rm ta}} r_{\rm inf}^3 \rho_{\rm tot} \quad \text{where} \quad \eta_{\rm ta} \simeq 1.086\,. \tag{1}$$

As time goes on, the plasma gets diluted and $r_{\rm inf}$ increases as $T^{-4/3}$ with T the plasma temperature. The smaller T, the larger the sphere of influence.

[1] For a discussion of PBHs as DM and related bounds on $f_{\rm BH}$, see for instance [9–11].

2.2 Onion-shell dark matter profile prior to collapse

WIMPs are in complete thermodynamical equilibrium with the surrounding plasma at early times. As T drops below the WIMP mass m_χ, the particles annihilate with each other. They eventually freeze-out when the annihilation rate becomes negligible with respect to the expansion rate. However, the numerous collisions of the DM species with the plasma constituents allow for thermal contact to remain established. A WIMP that would feel the gravitational pull of a PBH is prevented from falling onto it by the collisions it undergoes with the plasma.

The thermalization of DM with the plasma stops at kinetic decoupling, when WIMPs essentially cease to collide onto the plasma and to exchange energy with it. They can stream freely afterwards. At kinetic decoupling, all the WIMPs inside the sphere of influence start orbiting around the PBH. As time goes on, the sphere of influence grows and WIMPs located farther from the black hole get trapped, hence an onion-like structure for the DM pre-collapse density profile

$$\rho_i(r_i) \simeq \begin{cases} \rho_i^{\rm kd} & \text{if } r_i \leq r_{\rm kd}\,, \\ \rho_i^{\rm kd}\,(r_i/r_{\rm kd})^{-9/4} & \text{if } r_{\rm kd} \leq r_i \leq r_{\rm eq}\,. \end{cases} \tag{2}$$

At kinetic decoupling, the cosmological DM density is $\rho_i^{\rm kd}$ while the radius of the PBH sphere of influence is $r_{\rm kd}$. At matter-radiation equality, that radius is $r_{\rm eq}$ and the accretion of DM species stops to be considered as the radiation era comes to an end.

2.3 Orbital kinematics

DM particles feel only the gravitational pull of the PBH. Their trajectories are determined in the framework of classical mechanics and Newtonian gravity. Using the reduced orbital variables $\tilde{\boldsymbol{r}} = \boldsymbol{r}/r_{\rm S}$ and $\boldsymbol{\beta} = \boldsymbol{v}/c$, where $r_{\rm S}$ is the PBH Schwarzschild radius and c the speed of light, we define the reduced energy and orbital momentum as

$$\tilde{E} = \frac{E}{m_\chi c^2/2} = \beta^2 - \frac{1}{\tilde{r}} \quad \text{and} \quad \tilde{\boldsymbol{L}} = \tilde{\boldsymbol{r}} \wedge \boldsymbol{\beta}\,. \tag{3}$$

These quantities are conserved along each orbit. The initial state of a WIMP that feels for the first time the gravitational pull of the PBH is specified by the radius $\tilde{r}_i$, the velocity β_i and the angle θ_i between the injection and radial directions. The particle is trapped provided that the parameter $u \equiv \beta_i^2 \tilde{r}_i$ is less than 1. It reaches the radius $\tilde{r}$ if $u \geq 1 - X$, where X stands for the ratio $\tilde{r}_i/\tilde{r}$. At radius $\tilde{r}$, its radial velocity β_r fulfills the equation

$$\sin^2\theta_i \; + \left\{\frac{\tilde{r}^2}{\tilde{r}_i^2\beta_i^2}\right\}\beta_r^2 = \frac{\tilde{r}^2}{\tilde{r}_i^2}\left\{1 + \frac{1}{\beta_i^2}\left(\frac{1}{\tilde{r}} - \frac{1}{\tilde{r}_i}\right)\right\} \equiv 1 - \mathcal{Y}_{\rm m}\,. \tag{4}$$

This relation is a definition for the quantity $\mathcal{Y}_{\rm m}$ which plays an important role in the post-collapse DM profile. Note for the moment that $\mathcal{Y}_{\rm m}$ cannot exceed 1 but can be negative. If so, the radial velocity β_r at the target radius $\tilde{r}$ does not vanish whatever the injection angle θ_i.

The DM mini-spike surrounding a PBH results from the collapse of the initial distribution (2). In the past literature, the infall was assumed to be purely radial [12, 16]. As showed in [14], the initial orbital momenta $\tilde{L} = \tilde{r}_i\beta_i \sin\theta_i$ of WIMPs turn out to play a crucial role. The initial DM velocities β_i follow the Maxwellian distribution $\mathcal{F}_{\rm MB}(\beta_i|\tilde{r}_i)$ whose dispersion velocity σ_i scales with $\tilde{r}_i$ like $\rho_i^{1/3}$ according to Liouville's theorem. At kinetic decoupling, the DM dispersion velocity $\sigma_{\rm kd}$ is directly related to the ratio $x_{\rm kd} \equiv m_\chi/T_{\rm kd}$, with $T_{\rm kd}$ the plasma temperature. At matter-radiation equality, the WIMP dispersion velocity has been redshifted down to $\sigma_{\rm eq}$.

2.4 Post-collapse density profiles – numerical results and discussion

The contribution of each WIMP to the mini-spike density inside the layer of radius $\tilde{r}$ and thickness $d\tilde{r}$ is proportional to the fraction $2dt/T_{\rm orb}$ of the orbital time spent inside it. The duration dt depends on the radial velocity β_r, which depends itself on the injection angle θ_i and on the parameter $\mathcal{Y}_{\rm m}$. The orbital period $T_{\rm orb}$ follows Kepler's third law of planetary motion. At fixed $\tilde{r}_i$ and β_i, it does not depend on θ_i. Equipped with all these notations, the post-collapse DM density at radius $\tilde{r}$ can be readily derived as the integral over the initial phase space

$$\rho(\tilde{r}) = \frac{4}{\tilde{r}} \iint \tilde{r}_i \, d\tilde{r}_i \, \rho_i(\tilde{r}_i) \times d\beta_i^2 \, \mathcal{F}_{\rm MB}(\beta_i|\tilde{r}_i) \times \left\{ \frac{1}{\tilde{r}_i} - \beta_i^2 \right\}^{3/2} \times \int_0^{\theta_i^0} \frac{d(-\cos\theta_i)}{\sqrt{\cos^2\theta_i - \mathcal{Y}_{\rm m}}} \, . \tag{5}$$

The upper bound θ_i^0 of the angular integral is equal to $\arccos(\sqrt{\mathcal{Y}_{\rm m}})$ if $\mathcal{Y}_{\rm m} \geq 0$, and to $\pi/2$ if $\mathcal{Y}_{\rm m} \leq 0$. In spite of its simplicity, the numerical integration of relation (5) turns out to be tricky. The angular integral diverges logarithmically when $\mathcal{Y}_{\rm m} = 0$. The Gauss-Legendre method is by far the most stable way to compute the final DM density $\rho(\tilde{r})$.

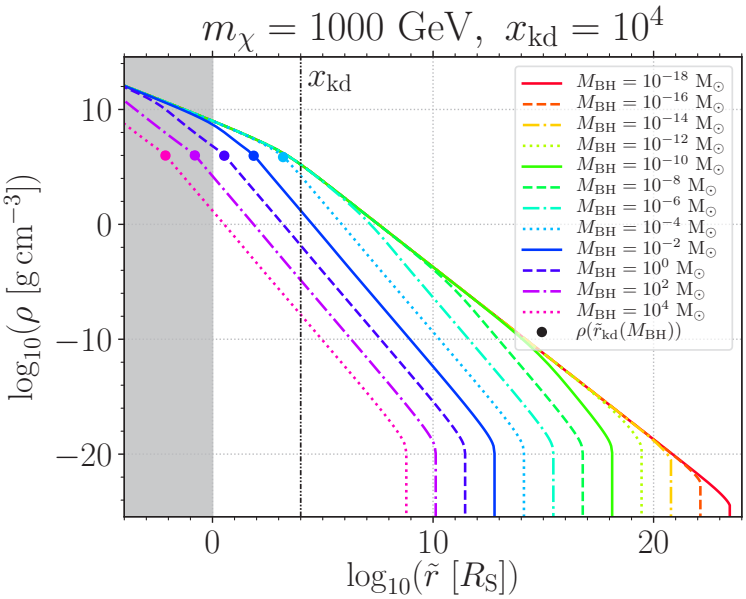

Figure 1. The density $\rho(\tilde{r})$ of the post-collapse DM mini-spike is plotted as a function of the reduced radius $\tilde{r}$ for various PBH masses $M_{\rm BH}$. The WIMP mass m_χ and kinetic decoupling parameter $x_{\rm kd}$ have been respectively set equal to 1 TeV and 10^4.

As featured in Fig. 1, the post-collapse DM profiles exhibit a rich diversity of behaviors depending on the PBH mass $M_{\rm BH}$. The mini-spikes extend from the Schwarzschild radius up to the radius of influence at matter-radiation equality $\tilde{r}_{\rm eq} \propto M_{\rm BH}^{-2/3}$. We first note that it is mandatory to let the parameter $\mathcal{Y}_{\rm m}$ be either positive or negative under the penalty of getting unphysical profiles. This point has been made clear for the first time in [13]. We then remark that the DM profiles are power laws $\rho(\tilde{r}) \propto \tilde{r}^{-\gamma}$ where the slope γ can take three distinct values, i.e. $\gamma = 3/4$, $3/2$ and $9/4$. We can actually delineate three regimes for the PBH mass.

• For low PBH masses, i.e. for $M_{\rm BH} \leq M_1$, the DM profiles are universal once the DM density ρ is expressed as a function of the reduced radius $\tilde{r}$. Below $\tilde{r} \simeq 0.088\, x_{\rm kd}$, the slope is $3/4$ and switches to $3/2$ above. In the case of Fig. 1, the value of M_1 is close to $10^{-13}\, M_\odot$.

• Above M_1 and below a critical mass M_2, which is equal to $3 \times 10^{-5}\, M_\odot$ in the configuration of Fig. 1, the inner profiles still exhibit a universal behavior with slopes $3/4$ and $3/2$. On the contrary, the outer parts of mini-spikes have slope $9/4$. There, the profiles can be obtained from one another by shifting them horizontally with $\tilde{r}$ scaling like $M_{\rm BH}^{-2/3}$. Up to a numerical factor of order 1, the post-collapse DM density at radius $\tilde{r}$ is actually equal to the cosmological DM density ρ_i at the exact cosmic time at which the reduced radius of the sphere of influence of the PBH is precisely equal to $\tilde{r}$.

• For heavy PBHs with masses larger than M_2, only the inner parts of mini-spikes exhibit a universal behavior with slope $3/4$. Going outward, the slope becomes $3/2$ and then $9/4$. Although no longer universal, the DM profiles can be shifted from one another with the same radial scaling as in the previous case. The transition between the slopes $3/2$ and $9/4$ occurs at the colored points of Fig. 1. These points are located at the radii of influence $\tilde{r}_{\rm kd} \propto M_{\rm BH}^{-2/3}$ and are aligned, ρ being given by the cosmological DM density $\rho_i^{\rm kd}$ at kinetic decoupling.

Most of the numerical results on the slopes have been derived in [17, 18]. The complex structure of mini-spikes has actually been understood analytically for the first time in [13] where details can be found. The DM profiles depend on three parameters, i.e. the WIMP mass m_χ and kinetic decoupling temperature $T_{\rm kd}$ as well as the PBH mass $M_{\rm BH}$. How the WIMP dispersion velocity σ_i just prior to infall compares to the escape velocity is crucial. The mass M_1 for instance is set by requiring that the dispersion velocity $\sigma_{\rm eq}$ at matter-radiation equality is equal to the escape velocity from radius $\tilde{r}_{\rm eq}$. Similarly, the mass M_2 is obtained by equating the dispersion velocity $\sigma_{\rm kd}$ at kinetic decoupling with the escape velocity from radius $\tilde{r}_{\rm kd}$.

3 Signatures and observational constraints

The DM mini-spikes around PBHs have kept the memory of how dense the universe was during the radiation era. The WIMPs inside them are highly packed and strongly self-annihilate. The DM skirts around PBHs are intense sources of γ-rays and neutrinos. They also inject energy inside the primeval plasma after recombination and re-ionize it, erasing anisotropies in the cosmic microwave background. The rate of WIMP annihilation inside a PBH mini-spike is given by

$$\Gamma_{\rm BH} = \frac{1}{2}\langle\sigma_{\rm ann} v\rangle \left\{\frac{\rho_{\rm sat}}{m_\chi}\right\}^2 r_{\rm S}^3 \int_1^{\tilde{r}_{\rm eq}} 4\pi\tilde{r}^2 {\rm d}\tilde{r} \left\{\frac{\rho(\tilde{r})}{\rho_{\rm sat}}\right\}^2 , \tag{6}$$

where $\langle\sigma_{\rm ann} v\rangle$ is the WIMP annihilation cross-section. Since matter-radiation equality at $t_{\rm eq}$, WIMPs have been annihilating and their density at cosmic time $t_{\rm U}(z)$ cannot exceed a maximal value $\rho_{\rm sat}$ set by the ratio $m_\chi/(\langle\sigma_{\rm ann} v\rangle\, \tau)$, with $\tau = t_{\rm U}(z) - t_{\rm eq}$. At fixed $\rho_{\rm sat}$, we observe that $\Gamma_{\rm BH}$ scales like $M_{\rm BH}^3$ for light PBHs, and like $M_{\rm BH}$ for heavy ones. In these regimes, $\Gamma_{\rm BH}$ is respectively proportional to $\langle\sigma_{\rm ann} v\rangle$ and $\langle\sigma_{\rm ann} v\rangle^{1/3}$. Note that $\Gamma_{\rm BH}$ depends on the redshift z through cosmic time $t_{\rm U}(z)$. The smaller the redshift, the smaller the annihilation rate.

The DM mini-spikes yield a non-negligible contribution to the extragalactic γ-ray background. Since this isotropic emission has been measured by the Fermi satellite, upper limits on the fraction $f_{\rm BH}$ of DM in the form of PBHs can be derived, as shown in Fig. 2. The complete analysis is quite involved insofar as it requires the modeling of the γ-ray diffuse emission from the Milky Way and of several extragalactic components. As pointed out in [17], this work has nevertheless been completed for decaying DM [19] with which mini-spikes present similarities. These can be seen as huge particles which would continuously decay. To be more specific, let us go a step further and consider a model where

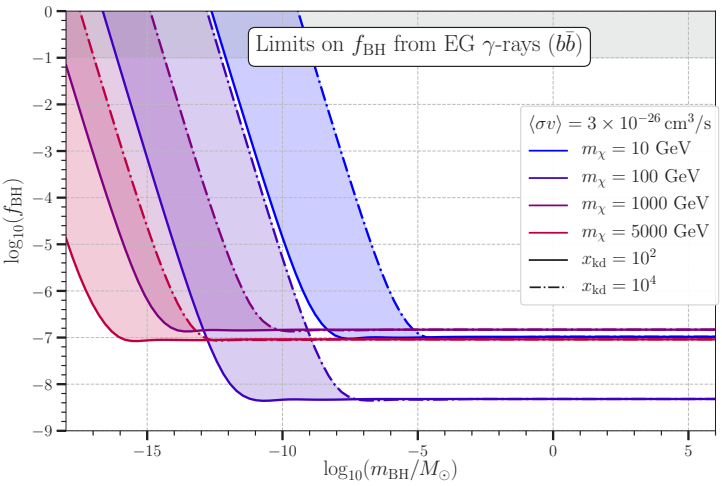

Figure 2. Upper bounds on the fraction $f_{\rm BH}$ as a function of PBH mass. WIMPs annihilate into $b\bar{b}$ pairs and the annihilation cross-section $\langle\sigma_{\rm ann}v\rangle$ has been set equal to its thermal value. Four values of the WIMP mass m_χ have been considered while the kinetic decoupling parameter $x_{\rm kd}$ has been varied from 10^2 to 10^4. These results refine those derived in [17, 18, 20, 21]

WIMPs decay or annihilate into $b\bar{b}$ pairs. The hadronization spectra of $b\bar{b}$ pairs induced by decay or annihilation at rest can be matched with each other if the decaying WIMP is twice as massive as the self-annihilating one. Therefore, we can match the local decay rate $\Gamma_{\rm dec} = \rho_{\rm DM}/(2m_\chi\tau_\chi)$ of WIMPs of mass $2m_\chi$, where τ_χ is the WIMP lifetime, with the local decay rate $\Gamma_{\rm spikes} = (\Gamma_{\rm BH} f_{\rm BH}\rho_{\rm DM})/M_{\rm BH}$ of spikes induced by the self-annihilation of WIMPs of mass m_χ. A lower limit $\tau_\chi^{\rm inf}$ has been set by [19] on the WIMP lifetime τ_χ. It can be recast into an upper bound on the fraction of PBHs

$$f_{\rm BH} \leq \left\{\frac{M_{\rm BH}}{2m_\chi}\right\}\left\{\frac{1/\tau_\chi^{\rm inf}}{\Gamma_{\rm BH}}\right\}. \tag{7}$$

These upper bounds have been plotted in Fig. 2 for four different WIMP masses. We notice the presence of a plateau for large values of $M_{\rm BH}$. In this regime, the limit does not depend on $x_{\rm kd}$ and is very stringent. PBHs would essentially be excluded, should the considered WIMPs exist. In the low-mass regime, the constraints on $f_{\rm BH}$ considerably weaken but are still strong in the asteroid window. Our results focus on an s-wave-dominated annihilation cross-section. They illustrate the difficulty in that case for DM to be made in comparable amounts of PBHs and DM particles, as already noticed by [12, 15, 17, 18].

Gravitational wave observatories will soon target merging events implying sub-solar objects. The detection of such mergers would be a smoking gun for the existence of PBHs. It is even conceivable that in the near future, the mass function of PBHs will be measured, i.e. that the fraction $f_{\rm BH}$ will be determined as a function of PBH mass. If so, we can invert the previous reasoning and constrain $\langle\sigma_{\rm ann}v\rangle$ at fixed m_χ, for instance from γ-ray observations. Using the limits on decaying DM derived in [19], we can directly recast relation (7) into an upper bound on $\Gamma_{\rm BH}$. This yields in turn an upper bound on $\langle\sigma_{\rm ann}v\rangle$ as shown in Fig. 3. Each line corresponds to a specific value of $f_{\rm BH}$. Notice how stringent the limits are. For illustration, let us consider a PBH fraction as small as 10^{-7}. WIMPs with thermal annihilation cross-section would be excluded in the mass range extending from 20 GeV to 1 TeV. The larger $f_{\rm BH}$, the

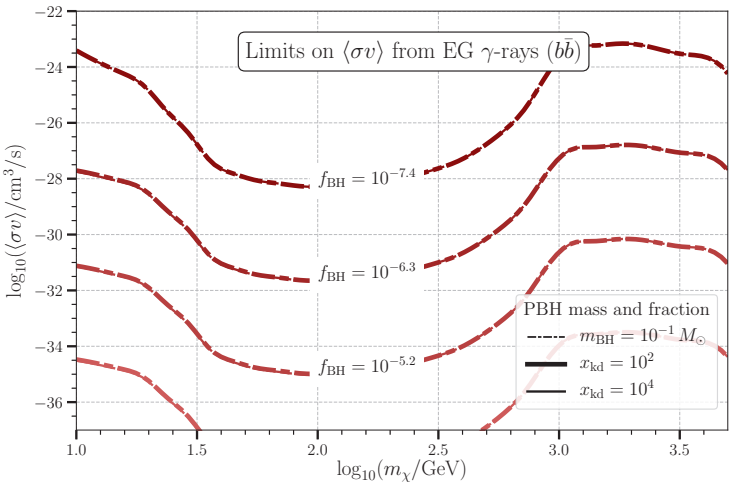

Figure 3. Upper limits on the annihilation cross-section of WIMPs as a function of their mass m_χ should PBHs with mass 0.1 $M_\odot$ be discovered. Each line is derived assuming a particular value for the fraction $f_{\rm BH}$ and recasting the limits on decaying DM from [19] into upper limits on $\Gamma_{\rm BH}$, and eventually on $\langle\sigma_{\rm ann}v\rangle$. Annihilations into $b\bar{b}$ are considered. The limits do not depend on the kinetic decoupling parameter $x_{\rm kd}$.

more stringent the upper bound on $\langle\sigma_{\rm ann}v\rangle$. A word of caution is mandatory though. We have concentrated so far on *s*-wave annihilating WIMPs. Our constraints would certainly relax for *p*-wave annihilation.

As a conclusion, our investigation of the properties of mixed DM, composed at the same time of PBHs and thermal DM species, has confirmed that it is difficult to make both components co-exist. We have also demonstrated that observations in the near future of mergers implying sub-solar objects would have considerable consequences on WIMP models.

Acknowledgements – One of us (P.S.) would like to thank warmly the organizers for the friendly, inspiring and exciting atmosphere of the RICAP-24 conference.

References

[1] Y.B. Zel'dovich, I.D. Novikov, The Hypothesis of Cores Retarded during Expansion and the Hot Cosmological Model, Soviet Ast. **10**, 602 (1967).

[2] S. Hawking, Gravitationally collapsed objects of very low mass, MNRAS **152**, 75 (1971). 10.1093/mnras/152.1.75

[3] B.J. Carr, S.W. Hawking, Black holes in the early Universe, MNRAS **168**, 399 (1974). 10.1093/mnras/168.2.399

[4] G.F. Chapline, Cosmological effects of primordial black holes, Nature **253**, 251 (1975). 10.1038/253251a0

[5] B.P. Abbott, R. Abbott, T.D. Abbott, M.R. Abernathy, F. Acernese, K. Ackley, C. Adams, T. Adams, P. Addesso, R.X. Adhikari et al., Observation of Gravitational Waves from a Binary Black Hole Merger, Phys. Rev. Lett. **116**, 061102 (2016), 1602.03837. 10.1103/PhysRevLett.116.061102

[6] S. Bird, I. Cholis, J.B. Muñoz, Y. Ali-Haïmoud, M. Kamionkowski, E.D. Kovetz, A. Raccanelli, A.G. Riess, Did LIGO Detect Dark Matter?, Phys. Rev. Lett. **116**, 201301 (2016), 1603.00464. 10.1103/PhysRevLett.116.201301

[7] S. Clesse, J. García-Bellido, The clustering of massive Primordial Black Holes as Dark Matter: Measuring their mass distribution with advanced LIGO, Physics of the Dark Universe **15**, 142 (2017), 1603.05234. 10.1016/j.dark.2016.10.002

[8] M. Sasaki, T. Suyama, T. Tanaka, S. Yokoyama, Primordial Black Hole Scenario for the Gravitational-Wave Event GW150914, Phys. Rev. Lett. **117**, 061101 (2016), 1603.08338. 10.1103/PhysRevLett.117.061101

[9] B.J. Carr, K. Kohri, Y. Sendouda, J. Yokoyama, Constraints on primordial black holes, Reports on Progress in Physics **84**, 116902 (2021), 2002.12778. 10.1088/1361-6633/ac1e31

[10] A.M. Green, B.J. Kavanagh, Primordial black holes as a dark matter candidate, Journal of Physics G Nuclear Physics **48**, 043001 (2021), 2007.10722. 10.1088/1361-6471/abc534

[11] B.J. Carr, A.M. Green, The History of Primordial Black Holes, arXiv e-prints arXiv:2406.05736 (2024), 2406.05736. 10.48550/arXiv.2406.05736

[12] B.C. Lacki, J.F. Beacom, Primordial Black Holes as Dark Matter: Almost All or Almost Nothing, ApJ **720**, L67 (2010), 1003.3466. 10.1088/2041-8205/720/1/L67

[13] M. Boudaud, T. Lacroix, M. Stref, J. Lavalle, P. Salati, In-depth analysis of the clustering of dark matter particles around primordial black holes. Part I. Density profiles, J. Cosmology Astropart. Phys. **2021**, 053 (2021), 2106.07480. 10.1088/1475-7516/2021/08/053

[14] Y.N. Eroshenko, Dark matter density spikes around primordial black holes, Astronomy Letters **42**, 347 (2016), 1607.00612. 10.1134/S1063773716060013

[15] J. Adamek, C.T. Byrnes, M. Gosenca, S. Hotchkiss, WIMPs and stellar-mass primordial black holes are incompatible, Phys. Rev. D **100**, 023506 (2019), 1901.08528. 10.1103/PhysRevD.100.023506

[16] K.J. Mack, J.P. Ostriker, M. Ricotti, Growth of Structure Seeded by Primordial Black Holes, ApJ **665**, 1277 (2007), astro-ph/0608642. 10.1086/518998

[17] S.M. Boucenna, F. Kühnel, T. Ohlsson, L. Visinelli, Novel constraints on mixed dark-matter scenarios of primordial black holes and WIMPs, J. Cosmology Astropart. Phys. **2018**, 003 (2018), 1712.06383. 10.1088/1475-7516/2018/07/003

[18] B. Carr, F. Kühnel, L. Visinelli, Black holes and WIMPs: all or nothing or something else, MNRAS **506**, 3648 (2021), 2011.01930. 10.1093/mnras/stab1930

[19] S. Ando, K. Ishiwata, Constraints on decaying dark matter from the extragalactic gamma-ray background, J. Cosmology Astropart. Phys. **2015**, 024 (2015), 1502.02007. 10.1088/1475-7516/2015/05/024

[20] E.U. Ginés, O. Mena, S.J. Witte, Revisiting constraints on WIMPs around primordial black holes, Phys. Rev. D **106**, 063538 (2022), 2207.09481. 10.1103/PhysRevD.106.063538

[21] P. Chanda, J. Scholtz, J. Unwin, Improved constraints on dark matter annihilations around primordial black holes, Journal of High Energy Physics **2024**, 273 (2024), 2209.07541. 10.1007/JHEP07(2024)273